
Article:
Rayner, Peter J. orcid.org/0000-0002-6577-4117, Burns, Michael J. orcid.org/0000-0002-5569-1270, Olaru, Alexandra M. orcid.org/0000-0002-2244-1048 et al. (6 more authors) (2017) Delivering strong 1H nuclear hyperpolarization levels and long magnetic lifetimes through signal amplification by reversible exchange. Proceedings of the National Academy of Sciences of the United States of America. 2016-20457RR. E3188-E3194. ISSN 1091-6490

https://doi.org/10.1073/pnas.1620457114

Delivering Strong ^{1}H Nuclear Hyperpolarization Levels and Long Magnetic Lifetimes through Signal Amplification by Reversible Exchange

Peter J. Rayner, Michael J. Burns, Alexandra M. Olaru, Philip Norcott, Marianna Fekete, Gary G. R. Green, Louise A. R. Highton, Ryan. E. Mewis and Simon. B. Duckett*

Centre for Hyperpolarisation in Magnetic Resonance, Department of Chemistry, University of York, Heslington, YO10 5NY

Hyperpolarization turns typically weak NMR and MRI responses into strong signals so that ordinarily impractical measurements become possible. The potential to revolutionize analytical NMR and clinical diagnosis through this approach reflect this area's most compelling outcomes. Methods to optimize the low cost *para*hydrogen based approach signal amplification by reversible exchange (SABRE) with studies on a series of biologically relevant nicotinamides and methyl nicotinates are detailed. These procedures involve specific ^{2}H-labelling in both the agent and catalyst and achieve polarization lifetimes of *ca*. 2 minutes with 50% polarization in the case of 4,6-d_2-methylnicotinate. As a 1.5 T hospital scanner has an effective ^{1}H polarization level of just 0.0005% this strategy should result in compressed detection times for chemically discerning measurements that probe disease. To demonstrate this techniques generality, we exemplify further studies on a range of pyridazine, pyrimidine, pyrazine and isonicotinamide analogues that feature as building blocks in biochemistry and many disease treating drugs.

Hyperpolarization | SABRE | Catalysis | NMR | MRI

Introduction

Nuclear magnetic resonance (NMR) is one of the most powerful methods available to study materials, whilst magnetic resonance imaging (MRI) is used widely in clinical diagnosis.(1) One route to improve the diagnostic capabilities of MRI involves monitoring *in vivo* changes in metabolite flux to non-invasively probe human physiology.(2) However, for reasons of low sensitivity, MRI detection needs to be coupled with approaches to increase signal strength such as hyperpolarization.(3) This process has been exemplified by studies on pyruvate which harnesses dissolution dynamic nuclear polarization (DNP)(4) to produce the signal strength necessary to track its metabolism.(5) Additionally, the related method of optical pumping noble gases, such as ^{129}Xe,(6) has provided the sensitivity needed to produce lung MR images that probe pulmonary disease.(5, 7) A recent report using γ-rays in conjunction with hyperpolarized ^{131}Xe has been used to image the distribution of a radioactive tracer at high sensitivity.(8)

*Para*hydrogen (p-H_2) induced polarization (PHIP)(9) is another hyperpolarization method that is showing great promise.(10, 11) p-H_2 is a unique hyperpolarized feedstock which has no magnetic moment and is not observable itself. Instead, a hyperpolarized agent is obtained when it adds to an unsaturated center as a consequence of this chemical change.(9) The resulting products' intrinsic magnetization, more commonly referred to as polarization, can lie so far from thermodynamic equilibrium that measurements which normally take months become possible in seconds.(12) However, this is only possible if the agent is detected before signal relaxation. Moreover, as the hyperpolarized magnetization is not replenished after relaxation the signal detection strategy needs careful consideration. Hence, imaging of hyperpolarized agents must be rapid compared to their relaxation rates. The development of this technique is, therefore fraught with experimental challenges as fresh samples are needed for each study. Furthermore, the use of NMR spectroscopy as an analytical tool would benefit substantially if materials can be rapidly characterized at lower concentrations than is currently possible.(13-15)

Significance

The study of molecules and materials is of great significance to both science and human welfare. The non-invasive techniques of nuclear magnetic resonance and magnetic resonance imaging reflect two of the most important methods to study them. However, both of these approaches are insensitive, and hyperpolarization methods to improve sensitivity are needed to access to new applications. The hyperpolarization approach Signal Amplification by Reversible Exchange (SABRE) is developed here to produce a signal whose strength is predicted to be 100,000 times larger than that which would be seen on a routine clinical MRI scanner under Boltzmann equilibrium conditions. By revealing the broad scope of this approach we demonstrate its potential for the future diagnostic detection of materials, metabolites and drugs.

In this study, we illustrate a number of new developments to improve the p-H_2 based method Signal Amplification By Reversible Exchange (SABRE).(16) This route shows great potential for enhancing both analytical NMR and clinical diagnosis in the future.(17-22) SABRE does not change the chemical identity of the agent it hyperpolarizes, but equilibrates polarization between p-H_2 and the selected agent through binding to an iridium center.(23) This simple process takes just a few seconds and is illustrated in Fig. 1.(24) Furthermore, the agents' hyperpolarization level can be maintained in low field when under p-H_2 as it can be continually repolarized.(24, 25) Consequently we predict that the future optimization of this method will be easier than that of many other approaches if we can deliver agents with high signal strengths and appropriately long-lived magnetization.

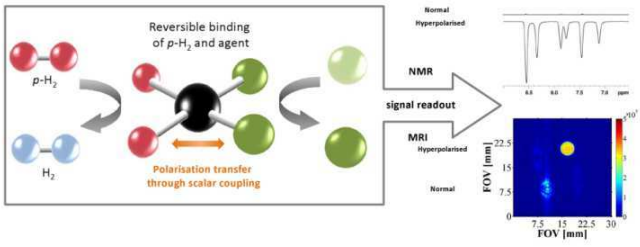

Fig. 1. Schematic representation of the SABRE effect

We present here a series of advances in substrate and catalyst design to meet these two challenges by reference to the substrates nicotinamide (**1**) and methyl nicotinate (**2**) before demonstrating the approach's wider applicability. These agents were selected because they exhibit low toxicity and play important roles in cellular biology.(26) The relaxation times and hyperpolarization levels of these agents are increased by the use of spin-dilution through ^{2}H-labelling, a strategy already used with DNP.(27) We also improve the lifetime of the agents' magnetization when bound to iridium through ^{2}H-labelling of the SABRE catalyst.(28) The hyperpolarization levels are increased still further with high p-H_2 pressures, and when a fully ^{2}H-labelled co-ligand is employed, 50% hyperpolarization is achieved in conjunction with magnetic-state lifetimes that approach 100 seconds in a ^{2}H-labelled nicotinate. By expanding the scope of this strategy to other target agents we show that a universal improvement in ^{1}H-hyperpolarization level and relaxation time is achieved. Single-scan MRI detection is then used to demonstrate that these improvements facilitate the acquisition of images whose intensity and contrast are vastly superior to those without hyperpolarization. Hence we are confident that the presented results reflect a series of key steps towards successful *in vivo* SABRE whilst serving to improve the methods potential as an analytical tool for NMR.

Results and discussion

The SABRE method starts by dissolving an agent (substrate) in a solvent that contains a metal based polarization transfer catalyst and then exposing it to p-H_2 for a few seconds in low magnetic field. The hyperpolarized agent can then be detected in a second step by NMR or MRI methods. Protio-nicotinamide (**1**) was one of the first substrates to be polarized by SABRE(16) and aspects of its ^{1}H, ^{13}C and ^{15}N signal enhancement have been previously communicated.(29-33).

In this work we undertake the SABRE process in the solvents methanol-d_4 or ethanol-d_6 at a field of 65 G unless otherwise stated and use a 400 MHz or 9.4 T field for the final measurement step. When **1** is hyperpolarized in this way through SABRE(30) in methanol-d_4 solution, as detailed in the supporting information, the signal for H-2 is ca. 650 times larger than that observed in a control measurement under Boltzmann conditions at a 9.4 T field. In contrast, the corresponding signals for H-4, H-5 and H-6 are 620, 190 and 590 times larger respectively than those of the H-2 control signal. Fig. 2-left illustrates a typical measurement. This signal intensity corresponds to detecting 2.1% H-2 polarization, created after a combination of just 7 seconds exposure to 3 bar of p-H_2 and three seconds for subsequent transfer into the measurement field. The corresponding polarization values in ethanol-d_6 range from 1.1 to 0.1% as detailed in Table 1. It is therefore straightforward to conclude that **1** is highly amenable to SABRE. Furthermore, according to the laws of signal averaging, if 31 seconds were needed to repeat each control measurement, it would take *ca*. 150 days of data collection to reproduce the previously detailed hyperpolarized result if a normal signal were to be employed.

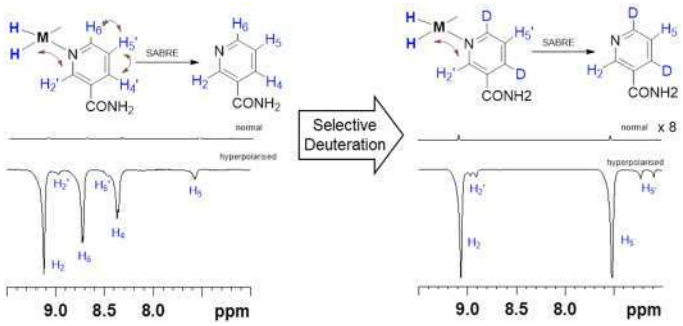

Fig. 2. SABRE hyperpolarization of nicotinamide: Left: Single scan ^{1}H NMR traces, with identical scaling, that illustrate nicotinamide (**1**) signals (as labelled) that result after SABRE (hyperpolarized) and when the polarization level matches that for thermodynamic equilibrium (normal). Right: Similar single scan ^{1}H NMR traces employing **1e** (Table 1); the normal trace has a x8 vertical expansion relative to the hyperpolarized trace (all measurements were performed in ethanol-d_6).

As we have indicated though, this signal gain must survive to the point of measurement. In methanol-d_4 solution, the four distinct protons resonances of **1**, H-2, H-4, H-5 and H-6, have T_1 values of 16.3, 11.3, 6.9 and 9.8 seconds at 9.4 T respectively (see Table 1, errors are <5% unless specified). These T_1 values change to 23.3 (50% increase), 6.7 (40% fall), 3.9 (45% fall) and 7.8 (20% fall) seconds respectively in ethanol-d_6 solution, and range from 10.7 to 6.5 seconds in D_2O solution. Hence these values are highly solvent dependent and not, at first glance, likely to be ideal for *in vivo* imaging; due to low SABRE efficiency in neat D_2O solutions the corresponding polarization levels are not reported.(34, 35)

Relaxation during SABRE catalysis

Examination of these NMR relaxation properties under SABRE conditions reveals that the observed T_1 values for the four proton signals of **1** reduce to just 6.2, 6.3, 3.7 and 3.8 seconds respectively in methanol-d_4. Furthermore, the H-2 T_1 value in ethanol-d_6 falls by 83% to 4.2 seconds thereby implying even faster signal destruction. During SABRE, rapid polarization transfer is beneficial in leading to a large signal gain but at high field, or without p-H_2, the catalyst clearly destroys the contrast agents' hyperpolarization by reducing T_1.(28, 36)

Using ^{2}H-labelling to reduce agent relaxation

Initially, we proposed to overcome these effects by using ^{2}H-labelling to extend the proton relaxation times of **1**.(29) Hence, nicotinamide derivatives **1a-1g** were prepared using the methods described in Fig. 3. These synthetic routes have been scaled to provide over 25 grams of the desired isotopologue and thus provide a robust platform to underpin any potential clinical/pre-clinical studies. Table 1 presents their SABRE performance and proton T_1 values, both with and without catalyst, at 9.4 T in methanol-d_4, ethanol-d_6 and D_2O solutions and clearly there is a beneficial extension in T_1.

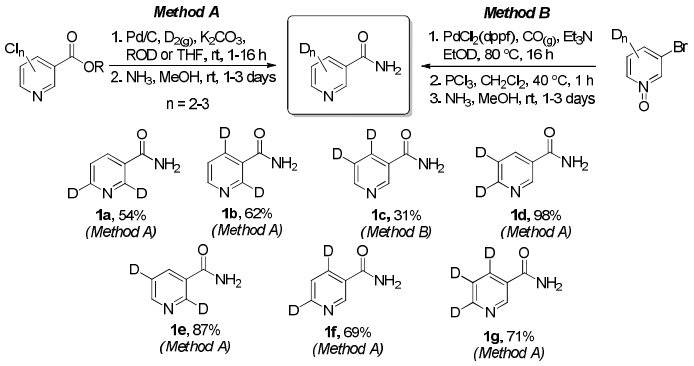

Fig. 3. Synthetic methods used to prepare agents **1a**-**1g**. Yields are isolated yields after column chromatography.

As these structures all contain fewer protons than **1**, they might be expected to achieve higher polarization levels under conditions when *p*-H_2 is the limiting reagent. However, substrate **1a**, whose *ortho* protons have been removed, gives low polarization under SABRE conditions. We conclude, therefore, that **1a** has polarization acceptor sites that are too magnetically isolated from the hydride ligands of the catalyst for effective SABRE transfer. In contrast, forms **1b-1g** all possess a proton adjacent to nitrogen, and based on the recent study by Tessari *et al.*, the relative position of the *ortho* proton to the ring substituent is unlikely to affect its coupling with the hydride ligand in the catalyst.(37) They should therefore all receive polarization at a similar rate and hence the poor performance of **1c** under SABRE must be a consequence of rapid relaxation. Hence we conclude that locating one proton next to the *N*-binding site (for strong coupling to the hydride ligands) and a longer-range coupling to a second longer-lived storage site is optimal.

This is reflected in the fact agents **1e** and **1f** have the largest average T_1 values of the series and perform best under SABRE. **1e** possesses a ^{4}J coupling between protons H-4 and H-6 that facilitates magnetization transfer between them and gives hyperpolarization levels of 2.7 and 3.2% respectively in methanol-d_4 (Fig. 1). For **1f**, the corresponding weaker ^{5}J coupling between protons H-2 and H-5 now results in each exhibiting a 4.1% hyperpolarization level. **1d**, with a ^{4}J, and **1b** with a ^{3}J coupling, and triply ^{2}H-labelled **1g** also perform less well than **1e** and **1f** which can readily be explained by their poor T_1 values.

Optimizing the SABRE catalysis of methyl nicotinate

As the amide protons of nicotinamide are likely to play a role in these relaxation processes the series of related methyl nicotinates **2a-2e**, shown in Table 2, were prepared and studied. The parent, protio-nicotinate **2**, proved to be superior to **1** under SABRE catalysis, with its four aromatic proton resonances showing an average polarization level of 2.7% in methanol-d_4 and 1.7% in ethanol-d_6 under our test; transfer to the methyl group is negligible. Furthermore, proton H-2 now has a T_1 value of 60 seconds in methanol-d_4, 49 seconds in ethanol-d_6 and 13.8 seconds in D_2O. In contrast, doubly ^{2}H-labelled 4,6-d_2-nicotinate (**2b**) has proton T_1 values in the absence of the catalyst for H-2 of 66 seconds and H-5 of 97.6 seconds in methanol-d_4. These drop to 46.2 and 62.7 seconds respectively in ethanol-d_6, but retain impressive values of 30.9 and 47.4 seconds in D_2O. As a consequence of these changes we boost the delivered SABRE polarization levels to 10.1% and 9.5% respectively in methanol whilst retaining an average hyperpolarization level of ca. 8.8% in ethanol-d_6. It proved possible to improve on these already impressive results by introducing a CD_3 label such that d_3-methyl 4,6-d_2-nicotinate (**2c**) exhibits T_1 values of 50.1 and 50.3 seconds in D_2O whilst achieving 7.2% polarization in ethanol-d_6.

Improving the SABRE catalyst through ^{2}H-labelling

The presence of the catalyst acts to reduce the measured T_1 values of the protons of the free substrate because the bound and free forms of the substrate are in dynamic exchange. Consequently the recorded protons' T_1 values reflect their appropriately weighted average. Hence, the T_1 value of a bound proton must be much smaller than the real value of the free material. We proved this by measuring the bound and free protons relaxation times at 263 K where ligand exchange is effectively quenched (see supporting information). We hypothesized that the slow rate of productive polarization transfer(23) means that any increase in the bound protons' relaxation times would be seen in an improved final agent polarization level. Conceptually, this could also be achieved by introducing ^{2}H-labelling into the *N*-heterocyclic carbene (NHC) ligand of the catalyst. Thus, we developed synthetic routes (see supporting information) to produce d_2-, d_{22}- and d_{24}-IMes ligands which were used to form the corresponding [IrCl(COD)(NHC)] catalyst (Fig. 4). The measured T_1 values of the protons in **2b** (bound and free) with these catalyst isotopomers, under 3 bar of H_2 or D_2, in methanol-d_4 solution are detailed in Table 3.

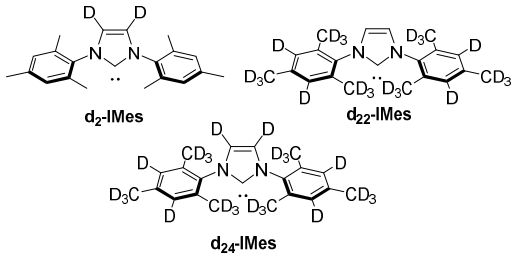

Fig. 4: ^{2}H-Labelled NHC ligands used for SABRE polarization with catalysts of type [IrCl(COD)(NHC)]

These data show that as predicted the T_1 values of the H-2 resonance in equatorially bound **2b** is increased by 36% on moving from H_2 to D_2 at 263 K. This confirms that coupling to the hydride ligands provide a significant route to relaxation. Furthermore, on comparing the d_2-, d_{22}- and d_{24}-IMes systems, there is an increase in both the bound T_1 and free substrate T_1 values. More importantly, when moving to 298 K where SABRE catalysis is conducted,(38) further increases in the protons' T_1 values free substrates are observed. Consequently we re-examined the SABRE efficiency of **2b** with these catalysts (Table 4). Both the effective T_1 relaxation times and polarization levels increased with the best performing catalyst, [IrCl(COD)(d_{22}-IMes)] giving average polarization levels of ca. 22.0% under 3 bar *p*-H_2 in both methanol-d_4 and ethanol-d_6 which reflects a 250% improvement in the latter case.

Effect of *p*-H_2 pressure on the level of SABRE

Up to this point we have conducted all SABRE catalysis under 3 bar pressure of *p*-H_2, which in our standard 5 mm J. Young's Tap NMR tubes reflects *ca.* 13-fold excess with respect to the substrate. Thus, if *p*-H_2 is the limiting reagent in this catalytic process, the reaction will ultimately progress to a point where normal H_2 (formed by conversion of *p*-H_2) is the dominant form in solution. Hence the SABRE hyperpolarization of **2b** was re-examined with [IrCl(COD)(d_{22}-IMes)] in methanol-d_4 and

ethanol-d_6 solution under 3.0-5.5 bar of p-H_2 (Fig. 5). In methanol-d_4 solution we see an increase in H-2 polarization to 26.4% and 28.5% at 4.0 and 5.5 bar respectively. A more significant effect is observed in ethanol-d_6 solution where a 55% increase in enhancement is observed at 5.5 bar of p-H_2 when compared to 3.0 bar. This results in a 41.7% polarization being measured on the H-2 site of **2b** under these conditions. These conditions are not used in the routine experiments we have described as they take the sample close to its safe pressure limit, and we would encourage any one repeating this work to take appropriate precautions.

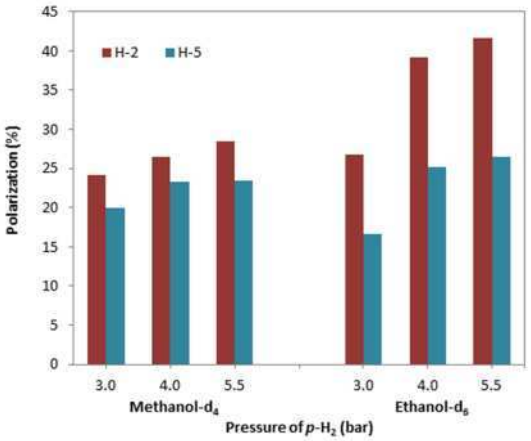

Fig. 5: Effect of p-H_2 pressure on the SABRE hyperpolarization of **2b** (4 eq.) with [IrCl(COD)(d_{22}-IMes)] (5 mM) in methanol-d_4 and ethanol-d_6.

Increasing SABRE hyperpolarization by using a co-ligand

Our final consideration in optimizing SABRE catalysis was to overcome the presence of multiple copies of the agent being attached simultaneously to a single iridium center and thus diluting any polarization coming from p-H_2. This would require a catalyst redesign, but if a co-ligand is added which cannot itself receive polarization a suitable test scenario can be established. Thus, SABRE hyperpolarization was conducted using a single equivalent of **2b** and three equivalents of methyl-2,4,5,6-d_4-nicotinate, relative to [IrCl(COD)(d_{22}-IMes)] under 5.5 bar p-H_2 pressure. This led to 50% polarization being achieved in the H-2 site of **2b**, with an average of 45% across the two sites. This is a truly remarkable result as it is delivered after just 10 seconds of SABRE. We validated this result on 3 samples that were each examined between 6 and 10 times. Hence we believe that this strategy reflects a compelling route to achieve high levels of hyperpolarization that could be improved still further by the use of even higher pressures and a superior catalyst.

Solvent effect on relaxation times

The efficiency of SABRE catalysis has been shown to be highly dependent on the solvent, with low hyperpolarization levels resulting in 100% D_2O solutions despite the development of water soluble catalysts.(34, 35, 39, 40) We suggest that hyperpolarization in an ethanol-d_6 solution followed by sample dilution to obtain a biocompatible bolus for injection reflects a sensible route to obtain the required signal strength for *in vivo* study. The T_1 values of **2b** were measured in ethanol-d_6–D_2O solvent mixtures (see supporting information). Despite the reduction in T_1 values for the H-2 and H-5 signals of **2b** in the mixed solvent systems, in a biocompatible mixture of 10% ethanol-d_6 in D_2O the T_1 value for H-5 remains above 30 seconds. Hence very high levels of hyperpolarization are expected to survive the point of injection. We have measured the T_1 values of H-2 and H-5 in **2b** in water (containing 5% D_2O) at 9.4 T, and they fall to 6.6 and 9.3 seconds respectively. These values suggest that a signal will be visible *in vivo* for at least 20 seconds, although if these approaches were to be used in drug/urine screening, or in analytical NMR more generally, there would be no issue with the decay of signal prior to measurement.

Expanding the range of substrates

We have also established the generality of this method by testing a range of additional substrates. To capture a suitable cross section of targets, we have employed materials bearing the nitrogen heterocyclic motifs, pyridazine (**3**), pyrimidine (**4**) and pyrazine (**5**) alongside isonicotinamide (**6**). The best performing isotopologues are presented in Fig. 6 and full data, including effective T_1 relaxation times in the presence of the catalyst can be found in the supporting information. In all cases, the relaxation times and polarization levels are increased. For 3,5-d_2-pyridazine (**3a**), the relaxation time is increased by 550% and the polarization level by 1630% relative to pyridazine (**3**). Similar effects were found for pyrimidine (**4**), where the deuterated isotopologue **4a** yields 4.8% polarization and a signal with a T_1 value of over 2 minutes. Comparison of pyrazine (**5**) to 2,5-d_2-pyrazine (**5a**) shows a relaxation time increase from 32.3 seconds to 86.2 seconds and a polarization level improvement from 3.3% to 11.6%. Finally, 2,5-d_2-isonicotinamide (**6a**) gives a *ca*. 5-fold improvement in T_1 and 80- and 6-fold improvements in polarization levels for H-3 and H-6 respectively over **6**.

These data show, therefore, that the strategy we detail to optimize the SABRE technology is applicable to a broad range of structural motifs and we suggest that most agents that have a need to be studied using either analytical NMR or in a clinical setting will benefit from isotope labelling. Table s5 in the supplementary information details the corresponding T_1 values in a 95% H_2O, 5% D_2O solution, with **2b**, **2c**, **3a**, **4a** and **5a** being the most likely to be detectable *in vivo*.

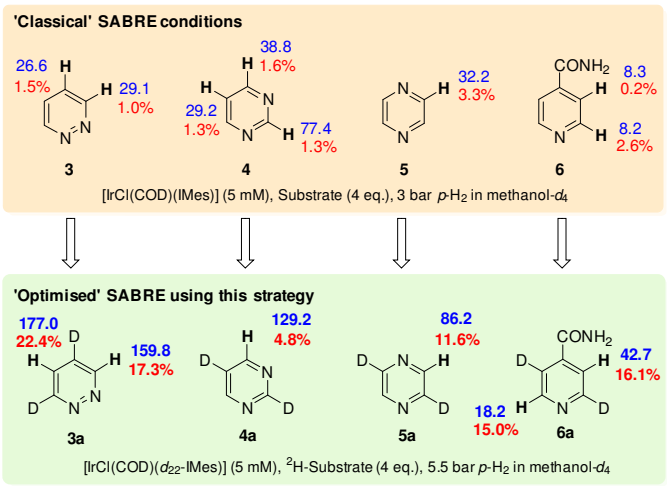

Fig. 6: $T_{1(\text{no cat})}$ values (in blue, seconds) and SABRE polarization levels (in red, percentage) of a range of substrates in methanol-d_4 solution to illustrate the general benefits of ^{2}H labelling.

Assessing the impact of these changes for MRI detection

Images of the resultant SABRE derived ^{1}H magnetization of **1** and **2**, and their better performing deuterated analogues, have been collected at 9.4 T in conjunction with a 100 mM substrate concentration in ethanol-d_6. Analogous results under reversible flow(41), where measurement-repeat is possible, are also detailed in the supporting information and confirm that deuteration not only improves the resultant image intensity relative to their parents but also extends the duration over which visible signals can be detected. The long T_1 values that these agents exhibit would normally inhibit standard pulse-recovery observations but are now expected to enable *in vivo* detection after transport to a region of clinical interest.

We have also been able to show that when high-contrast is desired, hyperpolarized signals can be observed in the presence of a water phantom whose signal can initially be suppressed to further improve the dynamic range of the image. In the cases of **1f** and **2b**, the hyperpolarized agents are visible 30 seconds after completion of the polarization step with superior image intensity to that of the residual water signal that survives its suppression. Furthermore, when **2b** was examined after polarization transfer by [IrCl(COD(d_{22}-IMes)] under 7 bar of p-H_2 the corresponding RARE(42) images of the same samples under normal conditions would take 9 and 40 days of continuous averaging in ethanol-d_6 and methanol-d_4 respectively to reproduce the hyperpolarized results (Fig. 7) that are collected in less than 20 seconds after the start of hyperpolarization. Hence we can conclude that the MRI assessment of these agents without hyperpolarization would be impractical. We also compared these data to that obtained for an excised spleen and noted a 30-fold S/N improvement relative to the tissue's H_2O signal.

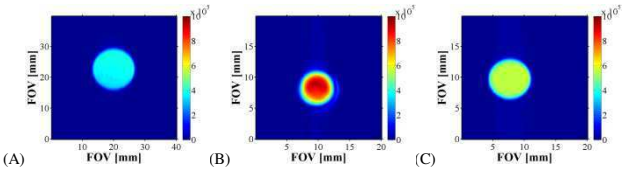

Fig. 7: Hyperpolarized images of methyl nicotinate using [IrCl(COD)(d_{22}-IMes)] under 7 bar p-H_2: (A) Control image of a tube of water; (B) SABRE hyperpolarized image of a sample of **2b** (100 mM in methanol-d_4); (C) analogous SABRE hyperpolarized image of a sample of **2b** (100 mM in ethanol-d_6). Image SNR values are 1586, 4085 and 2955 respectively. Data were acquired under identical conditions and results are plotted on the same scale.

Conclusions

The results presented here suggest that placing a proton next to nitrogen is most desirable for efficient magnetization transfer *via* SABRE while having an isolated proton environment is desirable for a long signal lifetime. In the case of nicotinamide (**1**) and methyl nicotinate (**2**), the deuterated forms that hyperpolarize optimally correspond to **1f** and **2b**. This is because polarization now flows optimally from the hydride ligands of the catalyst into receptor protons of the bound substrates that relax more slowly. Consequently, when [IrCl(COD)(IMes)] is used as the catalyst precursor, 10% polarization in **2b** is achieved for H-2 according to NMR spectroscopy measurement. However, as the catalyst also relaxes the hyperpolarization it creates ^{2}H-labelling of it is also highly beneficial. This simple change was found to double the level of delivered hyperpolarization to 22%. Increasing the p-H_2 pressure from 3 to 5.5 bar boosts this value to 41%, while 50% H-2 polarization in **2b** can be achieved when the co-ligand methyl-2,4,5,6-d_4-nicotinate is also present. Collectively these results reflect a strategy to create high levels of SABRE hyperpolarization that should be applicable to any target nucleus. Furthermore, by illustrating the success of this approach for a variety of agents we believe that we illustrate the generality of this strategy.

The resulting hyperpolarized and slowly relaxing agent's magnetization was also detected in a series of imaging experiments that served to establish that these performance improvements were maintained in MRI. **It must be borne in mind though that when measuring an MRI response, signal to noise and not the level of signal enhancement is critical. Hence the interplay between ^{1}H-concentration and hyperpolarization level must be taken into account.** An automated delivery system needs to be assembled if these results are to form the basis of future *in vivo* studies as the rapid in injection of these agents must follow sample dilution and catalyst removal steps. We are currently using this approach to optimally polarize the ^{13}C and ^{15}N nuclei of a range of substrates with long magnetization lifetimes. It should be noted that in recent reports hyperpolarized ^{15}N and ^{1}H NMR signals can be detected over 15 minutes after their creation by harnessing SABRE in conjunction with long-lived singlet states reflects a further route to extend this approach.(43, 44)

At a molecular level, we have developed and demonstrated a strategy to optimize the hyperpolarization levels of a biomarker and its relaxation characteristics. This has required the production of a range of ^{2}H-labelled substrates, and the selection of their optimal form based on their relaxation time and SABRE hyperpolarization level. We are also using this approach to improve NMR sensitivity for analytical purposes in a similar way.

Materials and Methods

Synthesis and Reactivity Studies All reactions utilizing air- and moisture-sensitive reagents were performed in dried glassware under an atmosphere of dry nitrogen. Dry solvents (THF, Toluene and DCM) were obtained from a Braun MB-SPS-800. For thin-layer chromatography (TLC) analysis, Merck pre-coated plates (silica gel 60 F254, Art 5715, 0.25 mm) were used. Column chromatography was performed on Fluka Silica gel (60 Å, 220-440 mesh). Deuterated solvents (methanol-d_4, ethanol-d_6 and D_2O) were obtained from Sigma-Aldrich and used as supplied. Detailed synthetic procedures and characterization data can be found in the supplementary material.

Hyperpolarization studies ^{1}H NMR spectra in addition to the relaxation data were measured on a Bruker 400 MHz spectrometer. SABRE hyperpolarization transfer experiments involved p-H_2 that was produced by cooling H_2 gas over Fe_2O_3 at 30 K. Samples contained 5 mM concentrations of the catalyst and between 5 and 20 equivalents of substrate relative to iridium in the specified solvent in a 5 mm NMR tube fitted with a J. Young's Tap. The resulting solutions were degassed prior to the introduction of p-H_2 at a pressure of 3 bar unless otherwise stated. Samples were shaken for 7 seconds in a specified fringe field of a 9.4 T Bruker Avance (III) NMR spectrometer for hyperpolarization transfer prior to being rapidly transported into the main magnetic field of the instrument for subsequent probing by NMR or MRI methods. The associated polarization transfer experiment data can be found in the supplementary material.

Statistical Analysis Errors have been calculated using the standard deviation formula, taking into account the limited number of population samples. Gaussian error propagation has been assumed (see supporting materials).

Acknowledgements

This work was supported by The Wellcome Trust (Grants 092506 and 098335), Bruker Biospin UK and the University of York. We also thank Professor V. H. Perry for useful discussions. Ryan Mewis is now based at Manchester Metropolitan University.

Author Contributions

P.J.R., M.J.B., A.M.O and S.B.D. conceived and designed the experiments. P.J.R, M.J.B and P.N synthesized and characterized non-commercial substrates and catalysts. P.J.R, M.J.B, P.N, M.F and R.E.M. performed and analyzed NMR measurements. A.M.O and L.A.R.H performed and analyzed the MRI experiments. P.J.R, M.J.B, A.M.O and S.B.D wrote the manuscript with interpretation and input from all authors. S.B.D. and G.G.R.G. provided supervision.

1. Kurhanewicz J*, et al.* (2011) Analysis of Cancer Metabolism by Imaging Hyperpolarized Nuclei: Prospects for Translation to Clinical Research. *Neoplasia* 13(2):81-97.
2. Gutte H*, et al.* (2015) The use of dynamic nuclear polarization (13)C-pyruvate MRS in cancer. *American journal of nuclear medicine and molecular imaging* 5(5):548-560.
3. Comment A & Merritt ME (2014) Hyperpolarized Magnetic Resonance as a Sensitive Detector of Metabolic Function. *Biochemistry* 53(47):7333-7357.
4. Ardenkjær-Larsen JH*, et al.* (2003) Increase in signal-to-noise ratio of > 10,000 times in liquid-state NMR. *Proceedings of the National Academy of Sciences* 100(18):10158-10163.
5. Lee Y (2016) Dissolution dynamic nuclear polarization-enhanced magnetic resonance spectroscopy and imaging: Chemical and biochemical reactions in nonequilibrium conditions. *Appl. Spectrosc. Rev.* 51(3):190-206.
6. Nikolaou P*, et al.* (2013) Near-unity nuclear polarization with an open-source Xe-129 hyperpolarizer for NMR and MRI. *Proceedings of the National Academy of Sciences of the United States of America* 110(35):14150-14155.
7. Nikolaou P*, et al.* (2014) XeNA: An automated 'open-source' Xe-129 hyperpolarizer for clinical use. *Magnetic Resonance Imaging* 32(5):541-550.
8. Zheng Y, Miller GW, Tobias WA, & Cates GD (2016) A method for imaging and spectroscopy using γ-rays and magnetic resonance. *Nature* 537(7622):652-655.
9. Bowers CR & Weitekamp DP (1987) Parahydrogen and synthesis allow dramatically enhanced nuclear alignment. *Journal of the American Chemical Society* 109(18):5541-5542.
10. Duckett SB & Mewis RE (2012) Application of Parahydrogen Induced Polarization Techniques in NMR Spectroscopy and Imaging. *Accounts of Chemical Research* 45(8):1247-1257.
11. Green RA*, et al.* (2012) The theory and practice of hyperpolarization in magnetic resonance using parahydrogen. *Progress in Nuclear Magnetic Resonance Spectroscopy* 67:1-48.
12. Anwar MS*, et al.* (2004) Preparing high purity initial states for nuclear magnetic resonance quantum computing. *Physical Review Letters* 93(4).
13. Beckonert O*, et al.* (2007) Metabolic profiling, metabolomic and metabonomic procedures for NMR spectroscopy of urine, plasma, serum and tissue extracts. *Nat. Protoc.* 2(11):2692-2703.
14. Reile I*, et al.* (2016) NMR detection in biofluid extracts at sub-mu M concentrations via para-H-2 induced hyperpolarization. *Analyst* 141(13):4001-4005.
15. Eshuis N*, et al.* (2014) Toward Nanomolar Detection by NMR Through SABRE Hyperpolarization. *Journal of the American Chemical Society* 136(7):2695-2698.
16. Adams RW*, et al.* (2009) Reversible Interactions with para-Hydrogen Enhance NMR Sensitivity by Polarization Transfer. *Science* 323(5922):1708-1711.
17. Frydman L (2009) Chemistry awakens a silent giant. *Nat. Chem.* 1(3):176-178.
18. Shchepin RV*, et al.* (2016) N-15 Hyperpolarization of Imidazole-N-15(2) for Magnetic Resonance pH Sensing via SABRE-SHEATH. *Acs Sensors* 1(6):640-644.
19. Logan AWJ, Theis T, Colell JFP, Warren WS, & Malcolmson SJ (2016) Hyperpolarization of Nitrogen-15 Schiff Bases by Reversible Exchange Catalysis with para-Hydrogen. *Chemistry-a European Journal* 22(31):10777-10781.
20. Truong ML*, et al.* (2015) N-15 Hyperpolarization by Reversible Exchange Using SABRE-SHEATH. *Journal of Physical Chemistry C* 119(16):8786-8797.
21. Zeng HF*, et al.* (2013) Optimization of SABRE for polarization of the tuberculosis drugs pyrazinamide and isoniazid. *Journal of Magnetic Resonance* 237:73-78.
22. Ducker EB, Kuhn LT, Munnemann K, & Griesinger C (2012) Similarity of SABRE field dependence in chemically different substrates. *Journal of Magnetic Resonance* 214:159-165.
23. Adams RW, Duckett SB, Green RA, Williamson DC, & Green GGR (2009) A theoretical basis for spontaneous polarization transfer in non-hydrogenative parahydrogen-induced polarization. *The Journal of Chemical Physics* 131(19):194505.
24. Hovener J-B*, et al.* (2013) A hyperpolarized equilibrium for magnetic resonance. *Nature Communications* 4:2946-2946.
25. Rovedo P*, et al.* (2016) Molecular MRI in the Earth's Magnetic Field Using Continuous Hyperpolarization of a Biomolecule in Water. *The Journal of Physical Chemistry B* 120(25):5670-5677.
26. MacKay D, Hathcock J, & Guarneri E (2012) Niacin: chemical forms, bioavailability, and health effects. *Nutrition Reviews* 70(6):357-366.
27. Allouche-Arnon H, Lerche MH, Karlsson M, Lenkinski RE, & Katz-Brull R (2011) Deuteration of a molecular probe for DNP hyperpolarization - a new approach and validation for choline chloride. *Contrast Media & Molecular Imaging* 6(6):499-506.
28. Mewis RE, Fekete M, Green GGR, Whitwood AC, & Duckett SB (2015) Deactivation of signal amplification by reversible exchange catalysis, progress towards in vivo application. *Chemical Communications* 51(48):9857-9859.
29. Mewis RE*, et al.* (2014) Probing signal amplification by reversible exchange using an NMR flow system. *Magnetic Resonance in Chemistry* 52(7):358-369.
30. Cowley MJ*, et al.* (2011) Iridium N-Heterocyclic Carbene Complexes as Efficient Catalysts for Magnetization Transfer from para-Hydrogen. *Journal of the American Chemical Society* 133(16):6134-6137.
31. Jiang W*, et al.* (2015) Hyperpolarized 15N-pyridine Derivatives as pH-Sensitive MRI Agents. *Scientific Reports* 5:9104.
32. Theis T*, et al.* (2015) Microtesla SABRE Enables 10% Nitrogen-15 Nuclear Spin Polarization. *Journal of the American Chemical Society* 137(4):1404-1407.
33. Shchepin RV, Barskiy DA, Mikhaylov DM, & Chekmenev EY (2016) Efficient Synthesis of Nicotinamide-1-15N for Ultrafast NMR Hyperpolarization Using Parahydrogen. *Bioconjugate Chemistry* 27(4):878-882.
34. Fekete M*, et al.* (2015) Utilisation of water soluble iridium catalysts for signal amplification by reversible exchange. *Dalton Transactions* 44(17):7870-7880.

35. Spannring P*, et al.* (2016) A New Ir-NHC Catalyst for Signal Amplification by Reversible Exchange in D2O. *Chemistry – A European Journal* 22(27):9277-9282.
36. Barskiy DA, Pravdivtsev AN, Ivanov KL, Kovtunov KV, & Koptyug IV (2016) A simple analytical model for signal amplification by reversible exchange (SABRE) process. *Physical Chemistry Chemical Physics* 18(1):89-93.
37. Eshuis N*, et al.* (2016) Determination of long-range scalar (1)H-(1)H coupling constants responsible for polarization transfer in SABRE. *Journal of magnetic resonance (San Diego, Calif. : 1997)* 265:59-66.
38. Lloyd LS*, et al.* (2014) Hyperpolarisation through reversible interactions with parahydrogen. *Cat. Sci. Tech.* 4(10):3544-3554.
39. Shi F*, et al.* (2016) Aqueous NMR Signal Enhancement by Reversible Exchange in a Single Step Using Water-Soluble Catalysts. *The Journal of Physical Chemistry C* 120(22):12149-12156.
40. Hövener J-B*, et al.* (2014) Toward Biocompatible Nuclear Hyperpolarization Using Signal Amplification by Reversible Exchange: Quantitative in Situ Spectroscopy and High-Field Imaging. *Analytical Chemistry* 86(3):1767-1774.
41. Mewis RE (2015) Developments and advances concerning the hyperpolarisation technique SABRE. *Magnetic Resonance in Chemistry* 53(10):789-800.
42. Hennig J, Nauerth A, & Friedburg H (1986) Rare Imaging - A Fast Imaging Method for Clinical MR. *Magnetic Resonance in Medicine* 3(6):823-833.
43. Roy SS, Norcott P, Rayner PJ, Green GGR, & Duckett SB (2016) A Hyperpolarizable H-1 Magnetic Resonance Probe for Signal Detection 15 Minutes after Spin Polarization Storage. *Angewandte Chemie-International Edition* 55(50):15642-15645.
44. Theis T*, et al.* (2016) Direct and cost-efficient hyperpolarization of long-lived nuclear spin states on universal N-15(2)-diazirine molecular tags. *Science Advances* 2(3).

Table 1. Hyperpolarization and T_1 data for nicotinamide (**1**) and the seven ^{2}H-labelled analogues **1a-1g**. SABRE catalysis performed with 5 mM [IrCl(COD)(IMes)] (IMes = 1,3-bis(2,4,6-trimethylphenyl)-imidazol-2-ylidene), 4 equivalents of agent, under 3 bar *p*-H_2 in methanol-d_4 or ethanol-d_6 at 298K. T_1 measurements without catalyst were on a degassed sample containing 20 mM of agent. Errors are <5% unless otherwise specified.

Agent	Methanol-d_4			Ethanol-d_6			D_2O
	Site $T_{1(\text{no cat.})}$ / s	Site $T_{1(\text{eff., with cat.})}$ /s	Polarization Level (%)	Site $T_{1(\text{no cat.})}$ / s	Site $T_{1(\text{eff., with cat.})}$ /s	Polarization Level (%)	T_1 / s
1 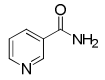	H-2: 16.3 H-4: 11.3 H-5: 6.9 H-6: 9.8	H-2: 6.2 H-4: 6.3 H-5: 3.7 H-6: 3.8	H-2: 2.1 H-4: 2.0 H-5: 0.6 H-6: 1.9	H-2: 24.3 H-4: 6.7 H-5: 3.9 H-6: 7.8	H-2: 4.2 H-4: 3.9 H-5: 2.4 H-6: 2.7	H-2: 1.1 H-4: 0.8 H-5: 0.1 H-6: 1.0	H-2: 10.7 H-4: 8.9 H-5: 6.5 H-6: 7.5
1a 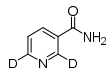	H-4: 11.2 H-5: 11.0	H-4: 5.8 H-5: 5.8	H-4: 0.2 H-5: 0.05	H-4: 6.1 H-5: 6.2	H-4: 3.8 H-5: 3.8	H-4: 0.1 H-5: 0.05	H-4: 11.2 H-5: 11.3
1b 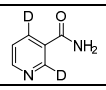	H-5: 14.5 H-6: 10.9	H-5: 5.8 H-6: 3.5	H-5: 2.4 H-6: 2.4	H-5: 7.3 H-6: 6.8	H-5: 5.1 H-6: 0.5	H-5: 0.3 H-6: 0.2	H-5: 12.2 H-6: 9.5
1c 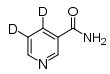	H-2: 14.8 H-6: 17.0	H-2: 3.7 H-6: 0.4	H-2: 1.7 H-6: 1.3	H-2: 13.5 H-6: 16.0	H-2: 3.2 H-6: 3.4	H-2: 0.9 H-6: 0.6	H-2: 39.4 H-6: 37.9
1d 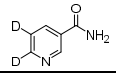	H-2: 8.1 H-4: 55.8	H-2: 6.7 H-4: 25.1	H-2: 2.1 H-4: 2.4	H-2: 8.1 H-4: 30.1	H-2: 3.3 H-4: 9.3	H-2: 0.6 H-4: 0.7	H-2: 13.0 H-4: 63.5
1e 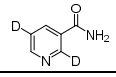	H-4: 63.5 H-6: 70.4	H-4: 18.9 H-6: 2.0	H-4: 2.7 H-6: 3.2	H-4: 28.0 H-6: 28.4	H-4: 14.6 H-6: 1.9	H-4: 1.9 H-6: 1.9	H-4: 51.8 H-6: 35.2
1f 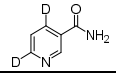	H-2: 26.8 H-5: 47.9	H-2: 7.9 H-5: 20.4	H-2: 4.1 H-5: 4.1	H-2: 22.2 H-5: 37.5	H-2: 8.2 H-5: 17.5	H-2: 2.0 H-5: 2.1	H-2: 37.1 H-5: 54.0
1g 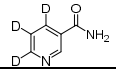	H-2: 45.7	H-2: 5.9	H-2: 2.1	H-2: 25.7	H-2: 3.8	H-2: 0.4	H-2: 28.5

Table 2. Hyperpolarization and T_1 data for methyl-nicotinate (**2**) and the four ^{2}H-labelled analogues **2a-2d**. SABRE catalysis performed with 5 mM [IrCl(COD)(IMes)] (IMes = 1,3-bis(2,4,6-trimethylphenyl)-imidazol-2-ylidene), 4 equivalents of agent, under 3 bar *p*-H_2 in methanol-d_4 or ethanol-d_6 at 298K. T_1 measurements without catalyst were on a degassed sample containing 20 mM of agent. Errors are <5% unless otherwise specified.

Agent	Methanol-d_4			Ethanol-d_6			D_2O
	Site $T_{1(\text{no cat.})}$ /s	Site $T_{1\ (\text{eff., with cat.})}$ /s	Polarization Level /%	Site $T_{1(\text{no cat.})}$ / s	Site $T_{1(\text{eff. with cat.})}$ /s	Polarization Level /%	T_1 / s
2 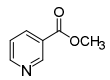	H-2: 59.8 H-4: 22.0 H-5: 12.6 H-6: 21.4	H-2: 4.9 H-4: 6.5 H-5: 3.6 H-6: 3.1	H-2: 3.7 H-4: 3.1 H-5: 1.3 H-6: 3.0	H-2: 48.9 H-4: 14.4 H-5: 8.1 H-6: 14.1	H-2: 8.0 H-4: 5.2 H-5: 4.9 H-6: 8.7	H-2: 2.6 H-4: 1.7 H-5: 0.7 H-6: 1.9	H-2: 13.8 H-4: 8.3 H-5: 6.2 H-6: 8.7
2a 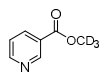	H-2: 67.2 H-4: 22.3 H-5: 12.4 H-6: 21.0	H-2: 5.3 H-4: 3.1 H-5: 7.0 H-6: 3.1	H-2: 5.8 H-4: 5.3 H-5: 1.4 H-6: 4.1	H-2: 31.0 H-4: 13.9 H-5: 7.9 H-6: 12.3	H-2: 14.9 H-4: 8.3 H-5: 4.9 H-6: 5.1	H-2: 1.5 H-4: 1.1 H-5: 0.5 H-6: 1.1	H-2: 37.1 H-4: 8.9 H-5: 6.8 H-6: 12.2
2b 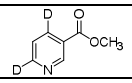	H-2: 65.7 H-5: 97.6	H-2: 5.8 H-5: 20.9	H-2: 10.1 H-5: 9.5	H-2: 46.2 H-5: 62.7	H-2: 6.8 H-5: 18.8	H-2: 9.3 H-5: 8.2	H-2: 30.9 H-5: 47.4
2c 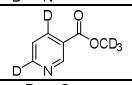	H-2: 116.0 H-5: 107	H-2: 6.6 H-5: 23.8	H-2: 9.5 H-5: 8.3	H-2: 49.8 H-5: 66.3	H-2: 5.5 H-5: 15.6	H-2: 7.5 H-5: 7.0	H-2: 50.1 H-5: 50.3
2d 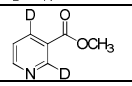	H-5: 26.0 H-6: 20.6	H-5: 5.5 H-6: 4.7	H-5: 3.7 H-6: 4.0	H-5: 16.7 H-6: 14.6	H-5: 5.5 H-6: 3.6	H-5: 2.7 H-6: 2.9	H-5: 15.7 H-6: 14.2
2e 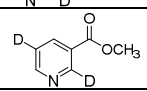	H-4: 94.3 H-6: 64.4	H-4: 28.2 H-6: 6.8	H-4: 11.0 H-6: 9.5	H-4: 61.2 H-6: 47.9	H-4: 24.6 H-6: 9.2	H-4: 6.2 H-6: 6.1	H-4: 44.2 H-6: 48.8

Table 3: Effective T_1 values for protons H-2 and H-5 in methyl-4,6-d_2-nicotinate **2b** (20mM loading), and the corresponding equatorial and axial ligands of the SABRE catalyst with [IrCl(COD)(NHC)] (where NHC = IMes, d_2-, d_{22}- or d_{24}-IMes, at 5 mM loading) and H_2 or D_2 (3 bar) in methanol-d_4 solution at 263 K.

NHC	**IMes** $T_{1(\text{eff., with cat.})}$/s				**d_2-IMes** $T_{1(\text{eff., with cat.})}$/s				**d_{22}-IMes** $T_{1(\text{eff., with cat.})}$/s				**d_{24}-IMes** $T_{1(\text{eff., with cat.})}$/s			
Gas	**H_2**		**D_2**		**H_2**		**D_2**		**H_2**		**D_2**		**H_2**		**D_2**	
2b	H-2:	10.6	H-2:	10.9	H-2:	13.1	H-2:	13.8	H-2:	13.5	H-2:	20.1	H-2:	12.1	H-2:	14.1
	H-5:	18.4	H-5:	18.3	H-5:	20.3	H-5:	25.3	H-5:	23.2	H-5:	23.7	H-5:	21.0	H-5:	30.9
Equatorially	H-2:	1.4	H-2:	1.9	H-2:	2.0	H-2:	1.5	H-2:	2.0	H-2:	2.6	H-2:	3.2	H-2:	2.3
Bound **2b**	H-5:	6.7	H-5:	5.6	H-5:	6.7	H-5:	6.5	H-5:	9.0	H-5:	7.3	H-5:	12.0	H-5:	10.5
Axially Bound	H-2:	1.9	H-2:	4.1	H-2:	1.7	H-2:	3.6	H-2:	2.5	H-2:	4.8	H-2:	1.7	H-2:	4.0
2b	H-5:	2.3	H-5:	2.4	H-5:	4.0	H-5:	2.7	H-5:	8.0	H-5:	3.8	H-5:	12.3	H-5:	10.1

Table 4: Effect of ^{2}H-labelling the catalyst on the effective T_1 values and polarization levels of H-2 and H-5 in **2b** under SABRE catalysis by [IrCl(COD)(NHC)] (where NHC = d_2-, d_{22}- or d_{24}-IMes) with 3 bar p-H_2 at 298 K.

NHC	**Methanol-d_4**				**Ethanol-d_6**			
	$T_{1(\text{eff., with cat.})}$/s		**Polarization /%**		**$T_{1(\text{eff., with cat.})}$/s**		**Polarization /%**	
d_2-IMes	H-2:	5.8	H-2:	10.1	H-2:	5.5	H-2:	9.3
	H-5:	20.9	**H-5:**	9.5	**H-5:**	15.6	**H-5:**	8.2
d_{22}-IMes	H-2:	7.7	H-2:	24.1	H-2:	7.7	H-2:	26.8
	H-5:	26.6	**H-5:**	19.9	**H-5:**	17.2	**H-5:**	16.6
d_{24}-IMes	H-2:	9.5	H-2:	18.6	H-2:	7.5	H-2:	13.3
	H-5:	33.5	**H-5:**	16.5	**H-5:**	19.3	**H-5:**	8.2